Characteristics of Cellular Infiltration into Posterior Vitreous in Eyes with Uveitis on the Classification Basis Assessed Using Optical Coherence Tomography

Matsumiya, Wataru ; Kusuhara, Sentaro ; Sotani, Noriyuki ; Kim, Kyung Woo ; Nishisho, Ryuto ; Sotani, Rei ; Imai, Hisanori ; Uji, Akihito ;…

(Citation)
Clinical Ophthalmology,17:165-174

(Issue Date)
2023-01-11

(Resource Type)
journal article

(Version)
Version of Record

Clinical Ophthalmology

Dovepress
open access to scientific and medical research

Open Access Full Text Article

ORIGINAL RESEARCH

Characteristics of Cellular Infiltration into Posterior Vitreous in Eyes with Uveitis on the Classification Basis Assessed Using Optical Coherence Tomography

Wataru Matsumiya[1], Sentaro Kusuhara[1], Noriyuki Sotani[1], Kyung Woo Kim[1], Ryuto Nishisho[1], Rei Sotani[1], Hisanori Imai[1], Akihito Uji[2], Makoto Nakamura[1]

[1]Department of Surgery, Division of Ophthalmology, Kobe University Graduate School of Medicine, Kobe, Japan; [2]Department of Ophthalmology, Kyoto University Graduate School of Medicine, Kyoto, Japan

Correspondence: Wataru Matsumiya, Department of Surgery, Division of Ophthalmology, Kobe University Graduate School of Medicine, 7-5-2 Kusunoki-cho, Chuo-ku, Kobe, 650-0017, Japan, Tel +81-78-382-6048, Fax +81-78-382-6059, Email ytkmatsu@med.kobe-u.ac.jp

Purpose: To evaluate the characteristics of posterior vitreous cells in patients with uveitis on the classification basis using spectral domain optical coherence tomography (SD-OCT).

Methods: In this retrospective chart review, all eyes were classified into three groups: infectious uveitis (IFU, n=7), noninfectious granulomatous uveitis (NIGU, n=13), and noninfectious nongranulomatous uveitis (NINGU, n=13). We measured the size, number, and density of vitreous hyperreflective particles in the posterior vitreous area that was defined as the space between the vitreous top and the internal limiting membrane on OCT. The correlations between vitreous haze and vitreous particles were also evaluated.

Results: Thirty-three eyes from 23 patients with active posterior uveitis were included. IFU had significantly more particles than NIGU and NINGU (P=0.03 and P<0.001, respectively). The vitreous particle density was higher in IFU than in NIGU and NINGU (P=0.03 and P=0.003, respectively). The mean largest particle size was greater in IFU and NIGU than in NINGU (P=0.01 and P=0.03, respectively). The median vitreous haze of 2+ in IFU, 1+ in NIGU and NINGU showed no significant difference among three groups (P=0.21). Conversely, the correlation of the largest particle size with vitreous haze was significant at ρ= 0.44 (P=0.01).

Conclusion: SD-OCT may be useful for assessing ocular inflammation based on morphological characteristics of vitreous particles on the uveitis classification basis.

Keywords: optical coherence tomography, OCT, vitreous cell, cell, hyperreflective particles, uveitis

Introduction

Uveitis can be caused by the numerous disorders associated with intraocular inflammation.[1] Some of these have infectious etiologies, and others are caused by systemic diseases, including autoimmune diseases. However, the causes can be unknown or unidentified in many cases. Globally, uveitis is also well known as a disease that potentially leads to blindness and accounts for 25% of total social blindness cases in the United States.[2,3] The classification of uveitis based on the degree of inflammation is crucial to evaluate treatment response during follow-up in clinical practice and to ensure standardization of evaluation to maintain the quality of clinical research in different sites.[4]

For management, uveitis is commonly etiologically classified into infectious uveitis (IFU) and nonIFU, followed by clinicopathological classification into granulomatous uveitis vs nongranulomatous uveitis based on ophthalmic examination such as the morphology of keratic precipitates.[5] Generally, Vogt–Koyanagi–Harada disease and sarcoidosis are classified into granulomatous uveitis. Granulomatous inflammation is a well-defined chronic or subacute inflammatory process, in which the activated macrophages play the main role and transform into epithelial cells.[6] In contrast, Behçet's disease was a representative disease of nongranulomatous uveitis. The main infiltrating cells in nongranulomatous

Received: 31 October 2022
Accepted: 29 December 2022
Published: 11 January 2023

inflammation are all kinds of leucocytes: polymorphonuclear neutrophils, eosinophils, basophils, lymphocytes, and macrophages. Thus, in the management of uveitis, it is important to classify nonIFU into granulomatous uveitis and nongranulomatous uveitis.[7]

In clinical practice, particular characteristics of intraocular cells, such as large cells, small cells, the number of cells, and cell shape, are the key factors that govern this uveitis classification. However, evaluations are made based on subjective examination by physicians, which may depend on their experience, environment, and equipment. Therefore, an objective method to evaluate characteristics of intraocular cells is required.

Recent advances in optical coherence tomography (OCT) have enabled visualization of intraocular inflammatory cells as hyperreflective particles.[8,9] As the resolution of OCT images has improved, some clinical studies have reported that SD-OCT can capture even subtle intraocular inflammation.[8,9] Especially in toxoplasmosis, even the time domain of OCT could detect intraretinal hyperreflective particles around active lesions. In SD-OCT, vitreous cellular infiltration are observed as vitreous hyperreflective particles.[10,11] Oréfice et al reported scattering hyperreflective particles in the vitreous of 18 of 24 eyes (75%) in patients with ocular toxoplasmosis.[11]

A previous study reported the use of an SD-OCT scoring system focusing the number of vitreous cells, where they were located, and retinal structure change such as disappearance of IS/OS line and destruction of the retinal layer structure in a mouse model of autoimmune uveoretinitis (EAU) to evaluate the severity of ocular inflammation with intraocular cellular infiltration.[12] This use led to the expectation that SD-OCT can evaluate the status of uveitis. Some recent studies also have shed light on the number or the density of vitreous cells as vitreous hyperreflective particles on OCT in patients with uveitis.[12–14] However, characteristics of cellular infiltration into posterior vitreous on the uveitis classification basis using OCT has not been studied well. Therefore, this study attempted to elucidate whether the morphological features of vitreal hyperreflective particles on SD-OCT differ among patients with IFU, noninfectious granulomatous uveitis (NIGU), and noninfectious nongranulomatous uveitis (NINGU).

Materials and Methods

Study Design and Participants

This retrospective comparative chart review enrolled Japanese patients from the Department of Ophthalmology, Kobe University Hospital, Japan. The Institutional Review Board at the Kobe University Graduate School of Medicine approved this study prior to data collection and allowed it to waive the need for informed consent. Instead, the review board accepted the opt-out recruitment approach as this was a noninterventional study with rigorous measurement to anonymize the personal information. This study was conducted according to the Declaration of Helsinki.

Patients in this study initially visited the Kobe University Hospital between January 2016 and January 2017. After a retrospective review, 33 eyes of 23 patients with active posterior or panuveitis were analyzed in this study. The eye with active ocular inflammation was defined as one that had at least one of the following findings: inflammatory chorioretinal or retinal vascular lesion, macular edema due to ocular inflammation, and vitreous haze grade of 2+ or higher with the Standardization of Uveitis Nomenclature (SUN) Working Group grade despite the treatment patients received. Patients with anterior or intermediate uveitis and cataract grade ≥3 (according to the Emery–Little classification) and without available good-quality OCT images were excluded. In addition, patients who had diabetic retinopathy, diabetic macular edema, vitreous hemorrhage, or age-related macular degeneration were excluded.

All eyes underwent slit lamp biomicroscopy, SD-OCT (Spectralis; Heidelberg Engineering, Heidelberg, Germany). All clinical data for this study were collected from clinical records, which included OCT imaging at the initial visit or any visits within one month from the initial visits with active inflammation before starting a new treatment or additional treatment at the Kobe University Hospital. After workup for ophthalmic and specific physical exams, including lab tests, multiplex PCR in aqueous humor, or vitreous samples, we classified all the eyes with defined uveitis into three groups based on clinical findings: IFU, NIGU, and NINGU. Regarding remaining uveitis as unclassified intraocular inflammation, we classified it into NIGU and NINGU based mainly on the morphological features such as keratic precipitates after we denied possible infectious etiology. According to vitreous haze grading, which was based on the scale developed by

Nussenblatt et al[15] and subsequently defined by the SUN working group,[12] we also assessed the vitreous haze score via slit lamp examination or fundus photography from the clinical records, as necessary.

Imaging Evaluation

In the evaluation of vitreal cellular infiltration, we selected the first 9-mm vertical and horizontal cross-sectional SD-OCT images through the fovea using B-scan averaging of >50 images. Next, after counting the number of hyperreflective particles, a vertical or horizontal scan (on which a larger number of particles was found) was analyzed to evaluate vitreal cellular infiltration (Figure 1A). Subsequently, the posterior vitreous area was measured, and the vitreous particle density was defined as "the particle number per vitreous area (particles/μm^2)" on OCT. In accordance with a previous report, the "posterior vitreous area" was measured as the space between the vitreous top and the internal limiting membrane after it was manually drawn using polygon selections tool in ImageJ software (Figure 1B).[12,14] We also measured the length of the vitreous particle ellipse in the maximum and minimum particles on imaging. For the measurement of the length of the vitreous particle ellipse, the grader manually chose three particles as the smallest and largest particles each on the OCT image. Both single and aggregated particles were considered as the largest particles. Then, both the vertical and horizontal lengths were measured for each particle.

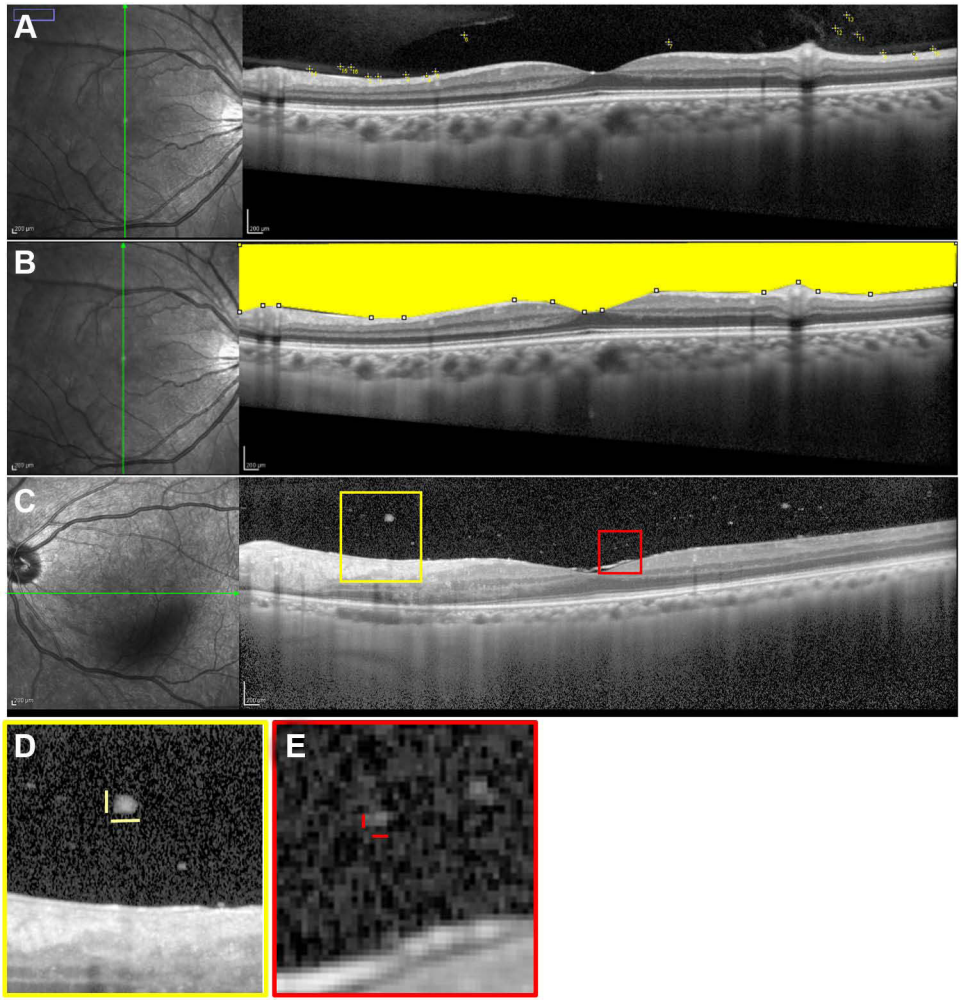

Figure 1 Measurement of the number of vitreous particles, vitreous particle density, and length of the largest and smallest vitreous particles on optical coherence tomography (OCT). On the vertical OCT scan image (**A**), 13 vitreous hyperreflective particles were counted manually in the vitreous space observed using OCT, with ImageJ software. Subsequently, on the same vertical OCT scan image (**B**), the vitreous area shown in yellow was defined as the space lying between the vitreous top and the internal limiting membrane, observed OCT. On another horizontal OCT scan image (**C**), the largest cell (vertical x horizontal shown as yellow bar: 64×138 μm) was shown in the yellow box (**D**) and the smallest cell (vertical x horizontal shown as red bar: 20×36 μm) in the red box (**E**). The longest length of largest and smallest cells are 138μm (**D**) and 36 μm (**E**), respectively.

Finally, the longest length of the vitreous particle ellipse in both the smallest and largest particles were obtained as "the length of particle" (Figure 1C–E). The data obtained from three independent graders, WM, KK, and NS, who were blinded to cases, were averaged and then used in analyses. All OCT images were imported in the ImageJ software version 1.50 (National Institutes of Health, Bethesda, MD, USA) to avoid image filtering; then, all evaluations were applied to each image. Imaging contrast was not adjusted before or after exporting images from the OCT system.

Outcomes

The primary outcomes were the total number of vitreal hyperreflective particles and the size of the smallest and largest particles among the IFU, NIGU, and NINGU groups.

Statistics Analyses

Given the fact that our data were derived from bilateral and unilateral eyes, generalized linear model (GLM) was appropriately applied in the case that inter-/intra-eye correlations were considered in comparison of data, instead of ANOVA. For analyses among the three groups, likelihood ratio tests were used for evaluation of model fitting. Simultaneously, comparison between two groups was also conducted with GLM. Statistical significance was defined at a *P*-value of <0.05. Especially, GLM model with Gaussian family and log link or with multinomial family and cumulative-logit link were utilized as necessary. Correlations of the four parameters related to vitreous particles with vitreous haze were evaluated using Spearman's coefficient of rank correlation. Intraclass correlation coefficients (ICCs) were measured to assess reliability among the three graders for all parameters. ICC was classified into poor, moderate, good, and excellent, based on each value.[16] Statistical analyses did not allow replacement of missing values in the parameters on OCT or vitreous haze. Given the aspect of exploratory research in this study, the number of cases was not defined before launching. All statistical analyses were conducted using R software (R Foundation for Statistical Computing, Vienna, Austria) with the graphical user interface EZR (Saitama Medical Center, Jichi Medical University, Saitama, Japan) and IBM SPSS Statistical Package for Social Sciences Version 25.0 (IBM Corporation, Armonk, NY, USA).

Results

Patient Characteristics

During the periods of chart review in this study, 94 eyes of 59 patients were identified as any type of uveitis. Among them, 64 eyes of 37 patients had active uveitis in posterior segment. After removing cases with poor OCT images or without OCT images in Heidelberg SD-OCT, 33 eyes of 23 patients were confirmed. The mean age of 23 patients with posterior or panuveitis was 54.4 ± 17.1 years (male:female ratio = 9:14). The IFU group had three eyes (43%) with cytomegalovirus (CMV) retinitis and one eye (14%) with varicella zoster virus (VZV)-associated uveitis, acute retinal necrosis caused by VZV, ocular toxocariasis, and ocular tuberculosis. CMV retinitis was the major cause in the IFU group. The NIGU group had four eyes (30%) with Vogt–Koyanagi–Harada (VKH) disease, two eyes (15%) with sarcoidosis, two eyes (15%) with retinal vasculitis from unknown etiology, and five eyes (38%) with unclassified intraocular inflammation. VKH accounted for one-third of the factors causing uveitis. The NINGU group had three eyes (23%) with uveitis caused by other systemic diseases, one eye (8%) with Fuchs' heterochromic iridocyclitis, and 9 eyes (69%) with unclassified intraocular inflammation. The baseline characteristics of patients in the present study are shown in Table 1.

The infectious group had a relatively higher vitreous haze grade than the other groups, but without significant difference among the three groups (*P*=0.21). The other variables were not significantly different among the groups. Representative cases are shown in Figure 2.

All data in included eyes with uveitis were shown in Supplementary Data.

Table 1 Baseline Characteristics of Patients

	Infectious	Noninfectious	
		Granulomatous	Nongranulomatous
Eye (n)	7	13	13
Patients (n)	6	7	10
Male (%)	5 (83.3%)	1 (14.3%)	6 (60.0%)
Age, years (Mean ±SD)	53.8±19.6	51.7±19.4	56.2±14.6
Baseline logMAR BCVA (Mean ±SD)	0.22±0.65	−0.05±0.20	0.06±0.18
Vitreous haze grade by SUN Criteria (Median [minimum-maximum])	2 (1–3)	1 (0.5–2)	1 (0.5–2)

Abbreviations: BCVA, best-corrected visual acuity; SUN, standardization of uveitis nomenclature; SD, standard deviation.

Number of Vitreous Hyperreflective Particles

The mean number of vitreous particles were 77.6±81.3, 18.7±6.7, and 13.6±8.5 particles in the IFU, NIGU, and NINGU groups, respectively (Figure 3A). The IFU group had significantly more particles than the NIGU and NINGU groups (P=0.03 and P<0.001, respectively; GLM). As assessed by the three graders, interclass correlation coefficients was excellent at 0.96.

Vitreous Particle Density

The mean vitreous area (μm^2), as observed on OCT, was 5.2±2.6 in the IFU group, 4.7±0.7 in the NIGU group, and 4.1 ±0.7 in the NINGU group (Figure 3B). Although the vitreous area in the IFU group was relatively larger than that in the

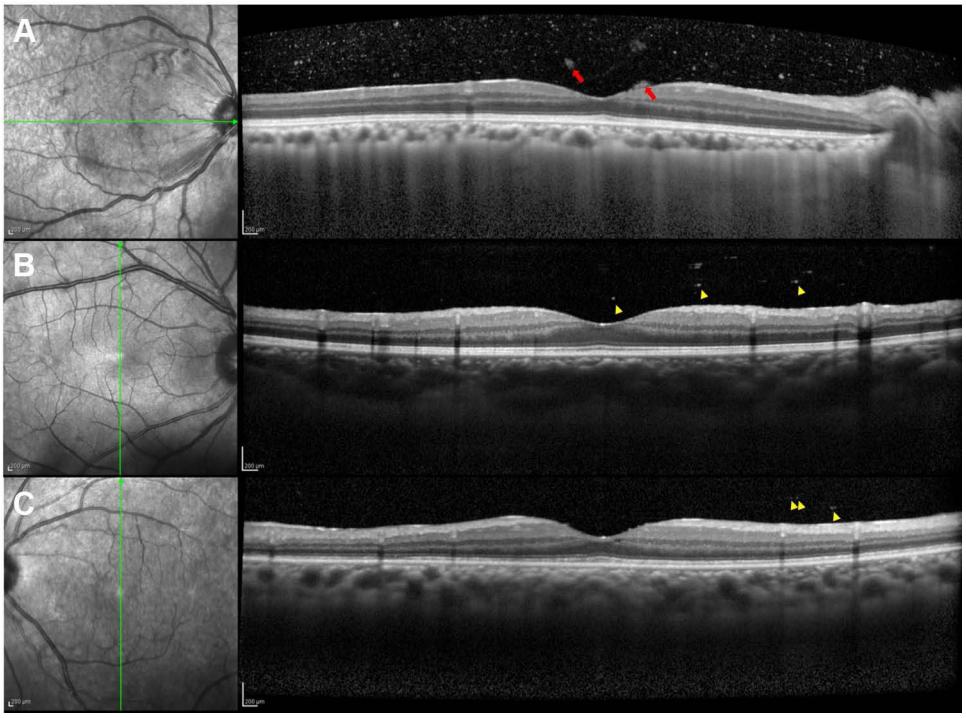

Figure 2 Representative cases with infectious uveitis, noninfectious granulomatous uveitis, and noninfectious nongranulomatous uveitis. (**A**) Numerous hyperreflective particles and few aggregated particles clots (red arrows) are shown in the horizontal OCT image, with cytomegalovirus retinitis as a cause of infectious uveitis. (**B**) Scattered vitreous particles and moderately sized particles without aggregating particles (yellow arrow heads) are observed in the vertical OCT image, with sarcoidosis as the cause of noninfectious granulomatous uveitis. (**C**) A few vitreous small particles (yellow arrow heads) are seen in the vertical OCT image, with psoriasis as a cause of noninfectious nongranulomatous uveitis.

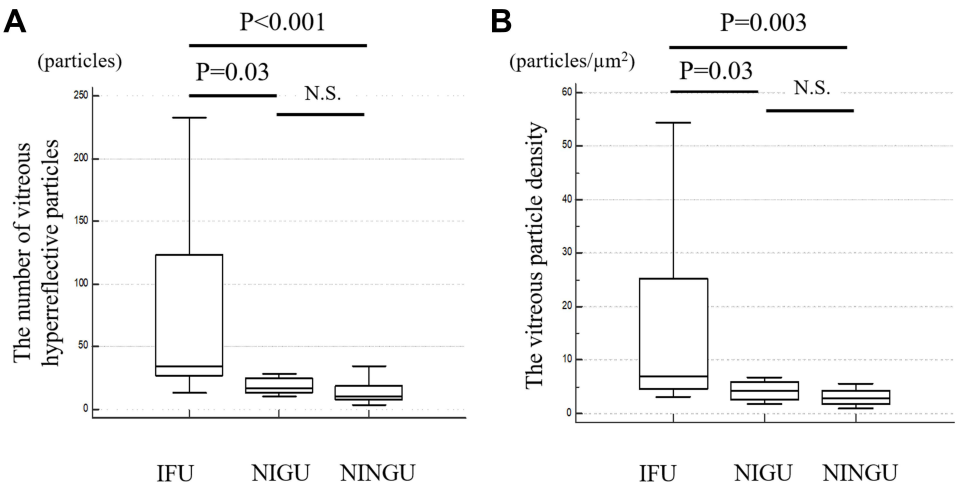

Figure 3 The number of vitreous particles as hyperreflective particles and vitreous particle density among three types of uveitis. (**A**) Patients with infectious uveitis had significantly greater number of vitreous particles than the other two types of uveitis. (**B**) Infectious uveitis had a significantly higher vitreous particle density than the other two types of uveitis.
Note: *P*-value was analyzed by generalized linear model.
Abbreviations: IFU, infectious uveitis; NIGU, noninfectious granulomatous uveitis; NINGU, noninfectious nongranulomatous uveitis.

other groups, no significant difference was noted among them. Vitreous particle densities (particles /μm^2) were 16.8±18.9 in the IFU group, 4.2±1.8 in NIGU group, and 3.3±2.0 in NINGU group, with a significant difference between the IFU and NIGU groups and IFU and NINGU (*P*=0.03 and *P*=0.003, respectively; GLM).

Length of the Smallest and Largest Particle

The mean length of the smallest particle was 19.8±5.3 μm in IFU group, 22.8±4.3 μm in NIGU group, and 22.8±5.8 μm in NINGU group. There were no significant differences in the length of the smallest particle among the three uveitis groups (Figure 4A). In contrast, the mean length of the largest particle was 146.0±70.1 μm in IFU group, 84.0±20.3 μm in NIGU group, and 60.7±38.5 μm in NINGU group (Figure 4B). The values in IFU and NIGU groups were larger than in NINGU group (*P*=0.014 and *P*=0.03, respectively; GLM). ICC among the results reported by the three graders was good at 0.85 for the size of the smallest particle and excellent at 0.91 for the largest particle.

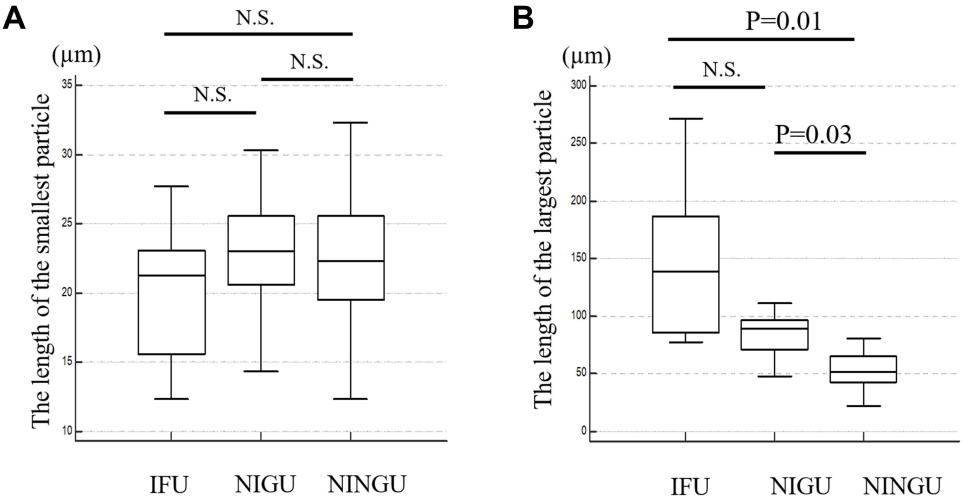

Figure 4 The length of of the smallest and largest particles among the three uveitis groups. (**A**) There are no significant differences among three types of uveitis in the length of the smallest particle. (**B**) The length of the largest particle was shorter in the noninfectious nongranulomatous uveitis group than in the other two groups.
Note: *P*-value was obtained by generalized linear model.
Abbreviations: IFU, infectious uveitis; NIGU, noninfectious granulomatous uveitis; NINGU, noninfectious nongranulomatous uveitis.

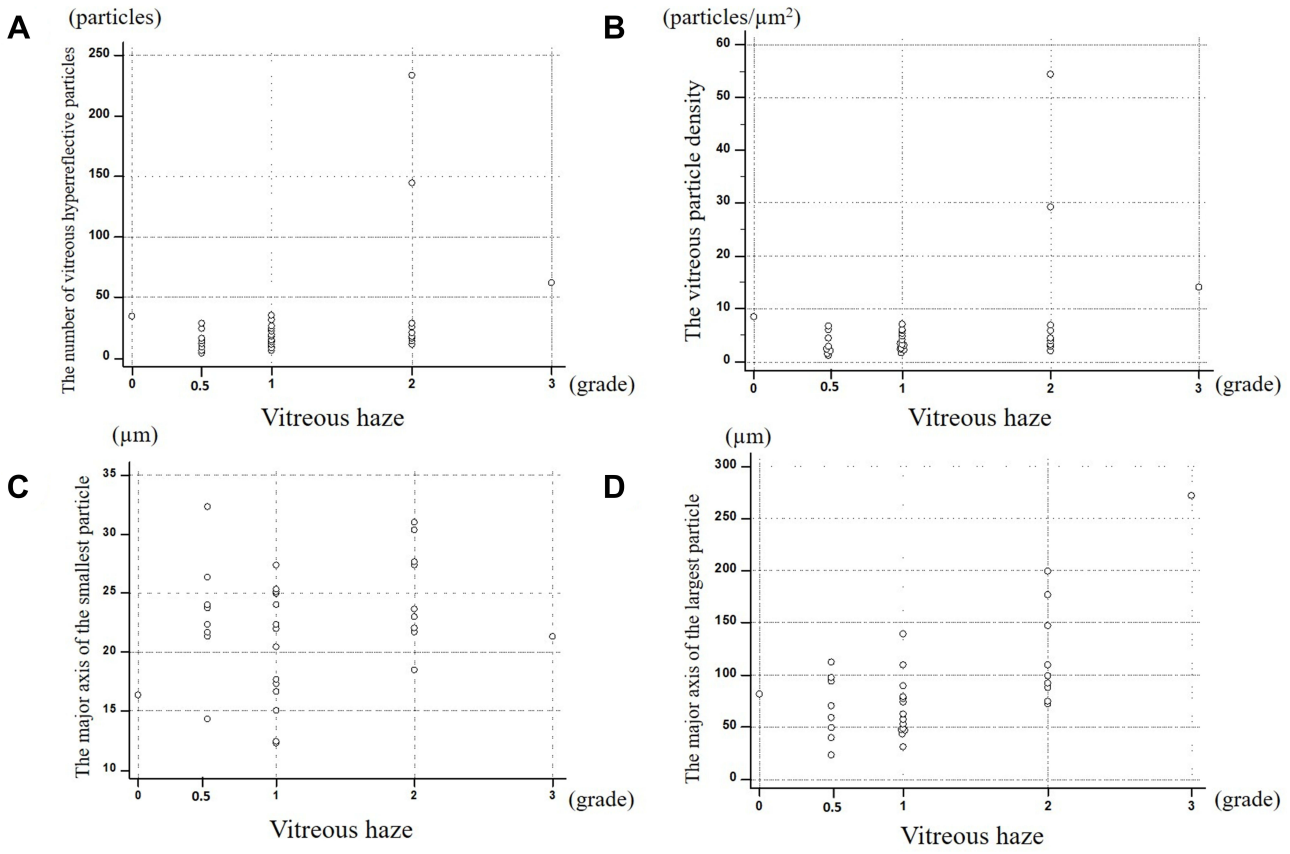

Figure 5 Correlation of each parameter related to vitreous particles with vitreous haze. Correlations between the number of vitreous hyperreflective particles (**A**), vitreous particle density (**B**), and the length of the smallest particle (**C**) were not significant at ρ=0.33 (*P*=0.06), ρ=0.29 (*P*=0.10), and ρ=0.16 (*P*=0.36), respectively. (**D**) Correlation of the length of the largest particle with vitreous haze was significant at ρ=0.44 (*P*=0.01).

Correlation of Each Parameter Related to Vitreous Particles with Vitreous Haze

Correlation of the length of the largest particle with vitreous haze was significant at ρ=0.44 (*P*=0.01) (Figure 5). In contrast, correlations among the number of vitreous hyperreflective particles, vitreous particle density, and the length of the smallest particle were not significant (*P*=0.06, *P*=0.10, and *P*=0.36, respectively).

Discussion

This study demonstrated significant differences in the number of vitreous hyperreflective particles, vitreous particle density, and the length of the largest particle on SD-OCT among the IFU, NIGU, and NINGU groups. In addition, there was a significant correlation between the length of the largest particle and vitreous haze. As a result, the IFU group had larger number of vitreous particles and higher vitreous particle density than NIGU and NINGU groups. The mean length of the largest particle was the longest in the IFU group, followed by that in the NIGU and NINGU groups. There were also significant differences between the IFU vs NINGU and NIGU vs NINGU groups. However, the mean length of the smallest particle did not differ significantly among the three uveitis groups.

It is well known that nongranulomatous inflammation can be associated with smaller lymphocytic cells rather than granulomatous inflammation, especially in the anterior chamber.[17] The SUN working group developed grading schemes for assessing the degree of inflammation in uveitis in 2005,[17] of which the grading in anterior chamber cells had a positive correlation with the severity of inflammation.

In uveitis, the mechanism by which inflammatory cells migrate into the eye is currently not fully elucidated; however, Whitcup et al demonstrated that in patients with uveitis, lymphocytes strongly expressing LFA-1 were present adjacent to the ICAM-1-expressing cells such as the RPE, glial cells, and vascular endothelium, which were induced by INF-γ, IL-1,

and TNF-α.[18] The recruitment and activation of more circulating monocytes and lymphocytes into the affected tissue are a by the activated T cells, followed by the production of various cytokines and chemokines including TNF-α and INF-γ, which are associated with regulating granulomatous immune responses. This is followed by the formation of epithelioid and multinucleated giant cells by the activated macrophages, which subsequently contribute to granuloma formation or cellular clots with aggregated cells.[19] Therefore, several immune cells are recruited and aggregated through the process of granulomatous inflammation.

Spectralis OCT, which we used as representative SD-OCT in this study, has an optical axial resolution of 7 μm/pixel and a digital axial resolution of 3.5 μm/pixel. This indicates that cells larger than the minimum size of lymphocytes, such as macrophages or monocytes, can be detected via OCT. Saito et al also indicated that highly reflective objects can be visualized by optical systems even if their size is smaller than the theoretical resolution.[9]

Therefore, this immunological theory could well explain the cellular behavior observed in our OCT analyses: larger number of particles and higher vitreous particle density on OCT were noted in IFU group than in NIGU and NINGU groups and larger size of particles on OCT were noted in IFU and NIGU groups than in NINGU group. Most infections are associated with granuloma formation; in particular, tuberculosis is the most common cause of granulomas. Besides tuberculosis, numerous other factors can also lead to ocular granulomatous inflammation, and these include infectious and noninfectious conditions such as syphilis, herpes viruses, CMV infection, toxoplasmosis, toxocariasis, sarcoidosis, multiple sclerosis, and VKH disease.[20] In the present study, the IFU group had several infectious diseases, as described above, which can cause granulomatous inflammation: CMV retinitis, VZV associated uveitis, acute retinal necrosis caused by VZV, ocular toxocariasis, and ocular tuberculosis. Especially, CMV retinitis was the majority of IFU groups in this study. As two out of three eyes with CMV infection showed moderate ocular inflammation at 1+ vitreous haze and one eye with CMV retinitis showed marked ocular inflammation with 2+ vitreous haze, CMV infection might induce multinucleated giant cells in infected cells.

The distinction between granulomatous vs nongranulomatous inflammation is useful in directing treatment and targeting a systemic workup, although granulomatous uveitis may initially present as nongranulomatous, and vice versa.[21]

Therefore, as the present study included the most representative infectious etiology in Japan,[22] the length of the largest particle may have the potential to help us classify uveitis into IFU and NINGU groups.

Moreover, granulomatous inflammation of the uvea can be even divided into three distinct morphologic categories: zonal, sarcoidal, and diffuse.[20] Tuberculous uveitis is histopathological representative of microbiologically proven cases and indicates zonal granulomatous inflammation of the uvea. Although fungal infections, foreign bodies, lymphomas, and tattoo-associated uveitis as well as sarcoidosis can be associated with granulomatous inflammation of the sarcoidal type. VKH disease is a representative case of diffuse granulomatous inflammation, which may have focal clusters of lymphocytes and epithelioid cells with pigment located between the retinal pigment epithelium and Bruch's membrane called as Dalen–Fuchs nodules.[20] The heterogeneity of infectious uveitis and the presence of subtypes of granulomatous inflammation may support our results that differences between IFU and NIGU groups in the length of the smallest and the largest particles were not significant, although the number of vitreous particles and vitreous particle density in IFU group were higher than those in the NIGU group.

Vitreous haze can reflect protein leakage into vitreous from retinal vessel and choroid due to a breakdown of the blood-retinal barrier caused by ocular inflammation. Given these complex mechanism of vitreous haze, the correlation of vitreous haze with vitreous cell might not be indicated using a simple linear formula; in addition, our results showed no significant correlation between vitreous haze and the number of vitreous cells. However, considering the pathological mechanism underlying the recruitment and accumulation of immune cells, the length of the largest particle may reflect the severity of ocular inflammation shown as vitreous haze.

There are some prior studies to evaluate viteral cellular infiltration and vitreous haze using OCT. One early study by Keane et al, reported a good correlation of OCT-derived measurements of vitreous signal intensity with clinical vitreous haze.[12] Moreover, Lee et al, reported an automated method based on deep learning to measure the number of vitreous hyperreflective foci and intensity of vitreous haze.[13] A recent report by Zicarelli et al, showed a significant correlation between vitreous cell density and the clinical grading of vitreous haze.[14] This result was not same as one in the present study. In contrast, it also reported that infectious uveitis had a higher cell density. That is comparable to the results of the

present study. In the present study, we focused on not only the number and density of vitreous particles, but also the size of them between three types of uveitis. In comparison with prior studies about OCT assessment for posterior ocular inflammation, that would be a potential novel point in the present study.

However, the present study had limitations in the study design owing to its retrospective nature and a relatively small number of subjects. Given the small sample size and inclusion of patients of a single race, this study did not always represent or cover all types of uveitis. Another limitation was that the measurement in this study was based on manual procedures despite using averaged data from three individuals. Regarding accuracy of measurement, automated or semi-automated measurement should be applied for future study. An additional limitation was the resolution of SD-OCT that did not allow us to depict all types of immune cells. Moreover, it was possible that resident macrophage cells like hyalocytes might be counted as inflammatory cells in the present study according to the previous report.[23] In addition, a single OCT scan might not always be able to depict the accurate morphology of vitreous cell. At last, as some of patients with uveitis at baseline were referred to our institution because they were refractory for topical steroid therapy, activity of ocular inflammation at baseline were already modified by prior therapies. Thus, a prospective study with a larger sample size will be required to confirm the results of the present study. However, our results suggested that SD-OCT could provide particular characteristics in vitreoretinal cellular infiltration to differentiate uveitis. The characteristics of vitreous particles such as the length of the largest particle as well as the number of vitreous particles and the vitreous particle density help classify uveitis better and may subsequently help physicians to manage uveitis.

To conclude, the number of vitreous particles, vitreous particle density, and length of the largest vitreous particle on OCT differed among the three types of uveitis. The length of the largest vitreous particle on OCT showed a significant correlation with vitreous haze. SD-OCT may be useful for classifying uveitis types and assessing the status of ocular inflammation based on differences in morphological characteristics and the number of vitreous particles.

Data Sharing Statement

All data relevant to the study are included in the article or uploaded as Supplementary Data. All data relevant to this study are included in the article.

Disclosure

The authors report no conflicts of interest in this work.

References

1. Zierhut M, Deuter C, Murray PI. Classification of uveitis–current guidelines. *J Classif Uveitis Curr Guidelines*. 2011. doi:10.17925/EOR.2007.00.00.77
2. Rothova A, Suttorp-van Schulten MS, Frits Treffers W, Kijlstra A. Causes and frequency of blindness in patients with intraocular inflammatory disease. *Br J Ophthalmol*. 1996;80(4):332–336. doi:10.1136/bjo.80.4.332
3. Durrani OM, Meads CA, Murray PI. Uveitis: a potentially blinding disease. *Ophthalmologica*. 2004;218(4):223–236. doi:10.1159/000078612
4. Bloch-Michel E, Nussenblatt RB. International Uveitis Study Group recommendations for the evaluation of intraocular inflammatory disease. *Am J Ophthalmol*. 1987;103(2):234–235. doi:10.1016/s0002-9394(14)74235-7
5. Rathinam SR, Babu M. Algorithmic approach in the diagnosis of uveitis. *Indian J Ophthalmol*. 2013;61(6):255–262. doi:10.4103/0301-4738.114092
6. Allegri P, Olivari S, Rissotto F, Rissotto R. Sarcoid uveitis: an intriguing challenger. *Medicina*. 2022;58(7):898. doi:10.3390/medicina58070898
7. Chan CC, Li Q. Immunopathology of uveitis. *Br J Ophthalmol*. 1998;82(1):91–96. doi:10.1136/bjo.82.1.91
8. Gallagher MJ, Yilmaz T, Cervantes-Castañeda RA, Foster CS. The characteristic features of optical coherence tomography in posterior uveitis. *Br J Ophthalmol*. 2007;91(12):1680–1685. doi:10.1136/bjo.2007.124099
9. Saito M, Barbazetto IA, Spaide RF. Intravitreal cellular infiltrate imaged as punctate spots by spectral-domain optical coherence tomography in eyes with posterior segment inflammatory disease. *Retina*. 2013;33(3):559–565. doi:10.1097/IAE.0b013e31826710ea
10. Oréfice JL, Costa RA, Oréfice F, Campos W, Da costa-lima D, Scott IU. Vitreoretinal morphology in active ocular toxoplasmosis: a prospective study by optical coherence tomography. *Br J Ophthalmol*. 2007;91(6):773–780. doi:10.1136/bjo.2006.108068
11. Oréfice JL, Costa RA, Scott IU, Calucci D, Oréfice F. Spectral optical coherence tomography findings in patients with ocular toxoplasmosis and active satellite lesions (MINAS Report 1). *Acta Ophthalmol*. 2013;91(1):e41–e47. doi:10.1111/j.1755-3768.2012.02531.x
12. Keane PA, Karampelas M, Sim DA, et al. Objective measurement of vitreous inflammation using optical coherence tomography. *Ophthalmology*. 2014;121(9):1706–1714. doi:10.1016/j.ophtha.2014.03.006
13. Lee H, Kim S, Chung H, Kim HC. Automated quantification of vitreous hyperreflective foci and vitreous haze using optical coherence tomography in patients with uveitis. *Retina*. 2021;41(11):2342–2350. doi:10.1097/iae.0000000000003190

14. Zicarelli F, Ometto G, Montesano G, et al. Objective quantification of posterior segment inflammation: measuring vitreous cells and haze using optical coherence tomography. *Am J Ophthalmol*. 2023;245:134–144. doi:10.1016/j.ajo.2022.08.025
15. Nussenblatt RB, Palestine AG, Chan CC, Roberge F. Standardization of vitreal inflammatory activity in intermediate and posterior uveitis. *Ophthalmology*. 1985;92(4):467–471.
16. Koo TK, Li MY. A guideline of selecting and reporting intraclass correlation coefficients for reliability research. *J Chiropr Med*. 2016;15(2):155–163. doi:10.1016/j.jcm.2016.02.012
17. Harthan JS, Opitz DL, Fromstein SR, Morettin CE. Diagnosis and treatment of anterior uveitis: optometric management. *Clin Optom*. 2016;8:23–35. doi:10.2147/opto.S72079
18. Whitcup SM, Chan CC, Li Q, Nussenblatt RB. Expression of cell adhesion molecules in posterior uveitis. *Arch Ophthalmol*. 1992;110(5):662–666. doi:10.1001/archopht.1992.01080170084029
19. Cavalcanti YV, Brelaz MC, Neves JK, Ferraz JC, Pereira VR. Role of TNF-Alpha, IFN-Gamma, and IL-10 in the Development of Pulmonary Tuberculosis. *Pulm Med*. 2012;2012:745483. doi:10.1155/2012/745483
20. Elnahry AG, Elnahry GA. Granulomatous uveitis. In: *StatPearls*. StatPearls Publishing Copyright © 2021, StatPearls Publishing LLC; 2021.
21. Herbort CP. Appraisal, work-up and diagnosis of anterior uveitis: a practical approach. *Middle East Afr J Ophthalmol*. 2009;16(4):159–167. doi:10.4103/0974-9233.58416
22. Sonoda KH, Hasegawa E, Namba K, Okada AA, Ohguro N, Goto H. Epidemiology of uveitis in Japan: a 2016 retrospective nationwide survey. *Jpn J Ophthalmol*. 2021;65(2):184–190. doi:10.1007/s10384-020-00809-1
23. Wang JM, Ong JX, Nesper PL, Fawzi AA, Lavine JA. Macrophage-like cells are still detectable on the retinal surface after posterior vitreous detachment. *Sci Rep*. 2022;12(1):12864. doi:10.1038/s41598-022-17229-5